DOI: https://doi.org/10.37434/tpwj2023.07.01

MATHEMATICAL MODELING OF THE IMPACT OF ELECTRODYNAMIC TREATMENT IN THE PROCESS OF ADDITIVE SURFACING ON THE STRESS-STRAIN STATE OF VOLUMETRIC PRODUCTS FROM ALUMINIUM-MAGNESIUM ALLOY

L.M. Lobanov[2], V.M. Korzhyk[1,2], M.O. Pashchyn[2], O.L. Mikhodui[2], P.R. Ustymenko[3], Zhang Yupeng[1], A.O. Alyoshin[2], O.M. Voitenko[2]

[1]China-Ukraine Institute of Welding, Guangdong Academy of Sciences,
Guangdong Provincial Key Laboratory of Advanced Welding Technology
Guangzhou, 510650, China
[2]E.O. Paton Electric Welding Institute of the NASU
11 Kazymyr Malevych Str., 03150, Kyiv, Ukraine
[3]National Technical University of Ukraine «Igor Sikorsky Kyiv Polytechnic Institute»
37 Peremohy Prosp., 03056, Kyiv, Ukraine

ABSTRACT

Combined 3D printing technology including a combination of additive (layer-by-layer) surfacing with electrodynamic treatment of deposited layer was considered. On the basis of mathematical modeling with the use of the Prandtl-Reiss ratio, on the example of aluminium-magnesium AMg6 alloy, the influence of the shape of the indenter for electrodynamic treatment on the distribution of basic parameters and components of the stress-strain state, in particular, the size of the zone of plastic deformations and stresses, depth and width of the contact interaction zone in a metal layer interacting with a roller-indenter moving along the normal to a layer at a speed of 1, 5 and 10 m/s across the thickness of the deposited layer was studied. It was established that the use of a roller with a contact surface, having a shape of a semi-circle, leads to an almost uniform distribution of compression stresses components in the deposited layer, the values of which can reach the yield strength of AMg6 alloy. The results of mathematical modeling give reasons to recommend the use of an electrode in the form of a semicircle (EC) for the development of combined technologies of 3D printing of volumetric metal products, which consist in combination of additive surfacing (WAAM, plasma, microplasma surfacing, etc.) of a volumetric metal product with electrodynamic treatment of each deposited layer.

KEYWORDS: 3D printing, additive surfacing, shaping technologies, electrodynamic treatment, aluminium alloy, impact interaction, mathematical modeling, residual stresses, plastic deformations, roller-indenter, generatrix, elastic-plastic environment

INTRODUCTION

3D printing (additive surfacing) is a method of shaping volumetric products on the base of digital models, the essence of which consists in layer-by-layer reproduction of objects. The use of technologies for 3D printing of parts based on aluminium alloys is promising in the engineering practice of manufacturing high-tech critical structures for the aircraft and space industries. The wide use of aluminium alloys is dictated by the fact that they have a high chemical resistance and a better ratio of strength to specific weight among most structural metal materials [1]. Usually, in the aerospace industry, AK12, AK94, 6061, 7075, AlSi12, AlSi10Mg alloys, etc. are used for 3D printing.

A promising direction of 3D printing is the use of welding technologies, such as layer-by-layer (additive) pulsed-arc surfacing of layers using wires as a shaping material (WAAM technology — Wire Direct Energy Deposition/Wire Arc Additive Manufacturing), as well as plasma (microplasma) layer-by-layer surfacing using powders or wires as additive materials, etc. [1, 2]. In these technologies, the material is deposited layer-by-layer by a robotic manipulator (or 3D positioner) according to the 3D model, as a result of which a three-dimensional workpiece is produced for further machining in a machine-tool with a numerical control (CNC) [3, 4].

It should be noted that, from the point of view of safe operation of aerospace engineering structures, the presence of even minimal defects in the structure of 3D printed parts of aluminium alloys is critically important for making a decision on the suitability of the specified technology. On the one hand, there is a need to refine the microstructure and improve the fatigue strength of parts produced by additive surfacing [4]. On the other hand, in the mentioned technologies

Figure 1. Process of 3D printing with plastic deformation of the deposited layer by electrodynamic treatment: *1* — torch for 3D printing; *2* — cylindrical electrode-indenter with the contact surface in the form of a straight line; *3* — printed layer of metal

there are risks of occurrence and the need in eliminating such a defect as discontinuity of material [5].

To solve these problems, electrodynamic treatment (EDT), which is one of the promising methods of influencing the structure of the surface layers of metal materials and regulating the stress-strain state (SSS), can be used [6]. EDT technology can be implemented in a combined process together with additive surfacing. The EDT process of the printed (deposited) layer is close to that in welding conditions, where the executive device (electrode system) moves behind the welding torch at a distance L_{EDT} behind it [7]. The values of L_{EDT} specify the temperature T_{EDT} of heating a printed layer as a result of the action of the thermal cycle of surfacing, at which its electrodynamic treatment can be carried out. At the same time, EDT can be applied to a printed layer, whose metal is at elevated or room temperatures.

Experimental and numerical methods of SSS analysis are used to study the EDT process. The work [8] considered the results of the numerical calculation of the process of impact interaction of the electrode-indenter with the plate of AMg6 during EDT based on the Prandtl–Reiss equations [9], which describe the movement of the medium in a planar two-dimensional formulation in the ANSYS/LS-DYNA software package.

The electrode-indenter for compacting a printed layer by the EDT method can be designed as a cylindrical roller with a different shape of the contact surface, for example, in the form of a straight line (Figure 1). The results of mathematical modeling of the impact of different structural forms of the indenter during EDT on residual welding stresses are presented in [10].

The results of [10] proved that a designed shape of the indenter during EDT has a significant impact on the distribution of residual welding stresses in the plate of AMg6 alloy. Control of welding stresses, including the formation of compressive stresses, is precisely one of the important tasks in the development of additive surfacing technologies. Considering the abovementioned, it should be noted that the shape of the contact surface of the indenter for EDT should affect the characteristics of the plastic deformation of the metal after 3D printing, which is determined by the formation of compressive stresses in it. Thus, optimization of the geometric shape of the contact surface of the roller-indenter for EDT, which performs the treatment of the deposited layer, can generally improve the mechanical characteristics of a printed metal.

The aim of the work is to evaluate, based on the mathematical modeling, the impact of the shape of the electrode-indenter on the distribution of components of plastic deformations and residual stresses during the formation of volumetric metal products in the combined process of "additive surfacing - layer-by-layer electrodynamic treatment".

CALCULATION (MATHEMATICAL) MODEL OF THE PROBLEM

Mathematical modeling of residual stress states after EDT of welded joints is considered in detail in [8]. The scheme of the EDT process of the plate metal after 3D printing is shown in Figure 2. During EDT, the electrodynamic pressure on the disc *2* of a non-ferromagnet (Figure 2, *a*) and the indenter *4* is the result of the interaction of eddy currents with the pulsed magnetic field of the inductor 1 when the contactor *K* starts the discharge cycle of the capacitor *C* [6].

Figure 2 shows that in the EDT process, the copper electrode-indenter *4* and the deposited layer *5* of AMg6 alloy with a thickness $\delta = 4$ mm and a width of 50 mm, which in the calculations is taken in the form of a plate located on a completely rigid surface (working table *6*), interact with impact. At the same time, the electrode-indenter moves in the direction (along the normal) to the plate *5* at a speed V_0. Geometric symmetry in modeling allows using only a half of the plate and indenter, located to the right of the line of electrodynamic pressure V_0 in Figure 2, *b*, *c*. In modeling, it is assumed that the cross-section of a printed layer does not exceed the cross-section of the plate.

Thus, the numerical calculation using a planar two-dimensional model in the Lagrangian setting will correspond to the modeling of the EDT process of the plate by electrode-indenter with a profiled contact surface in the form of a semicircle — EC (Figure 2, *b*) or in a planar shape (EP) (Figure 2, *c*). The difference between the two presented calculation schemes consists in the fact that the contact of EC surface and the plate occurs at a point (Figure 2, *b*), and the contact of EP surface and the plate occurs along the line (Figure 2, *c*).

The creation of a mathematical model of the process described above was carried out using a simplified two-dimensional (2D) planar setting. The problem was solved using the ANSYS/LS-DYNA software [8–10]. A planar two-dimensional finite element in the form of SOLID162 rectangle was used to construct the finite element mesh of the problem. Taken into account that the stress-strain state of solid bodies is considered in this problem, the computer modeling should be carried out using the Lagrangian approach [8–10]. As is known, the Lagrangian approach uses a moving finite-element mesh that is rigidly connected to the environment and deforms together with it.

The presence of the abovementioned described geometric symmetry of impact-interacting bodies allows considering only half of their cross-section relative to *OY* axis with the simultaneous imposition of the corresponding boundary conditions. These conditions include banning the movement of nodes of the finite element mesh (FEM) of bodies located on the axis of symmetry in the horizontal direction *OX*. The presence of the working table 6 in the scheme of electrodynamic treatment of the plate (Figure 2, *a*) is rational to be replaced by resting on an absolutely rigid base, which in the mathematical setting will be equivalent to banning movement in the vertical direction *OY* to the FEM nodes that belong to the lower surface of the plate *5*, which is in contact with the table.

A finite element with a maximum characteristic size of 0.1 mm was chosen to construct the finite element model of the plate and electrode-indenter. The constructed finite element models for both variants of the calculation scheme had the same number of finite elements (SOLID 162 type) — 4288 and the same number of nodes — 4514, where the electrode-indenter had 2688 elements and 2797 nodes, and the plate consisted of 1600 elements and 1717 nodes.

For numerical modeling of a high-speed impact process, a continuous model of the experimental medium was used [8–10]. The basis of the model is the hypothesis about the continuity of changes in the characteristics of the medium in space (coordinate, time), which allows recording the laws of conservation of mass, amount of motion and energy in the form of partial differential equations.

If we choose a Cartesian (rectangular) coordinate system to describe the adiabatic motion of an elastic-plastic medium with a density ρ (kg/m^3), then the system of the corresponding equations in the two-dimensional setting will have the form [9]:

The equation of continuity:

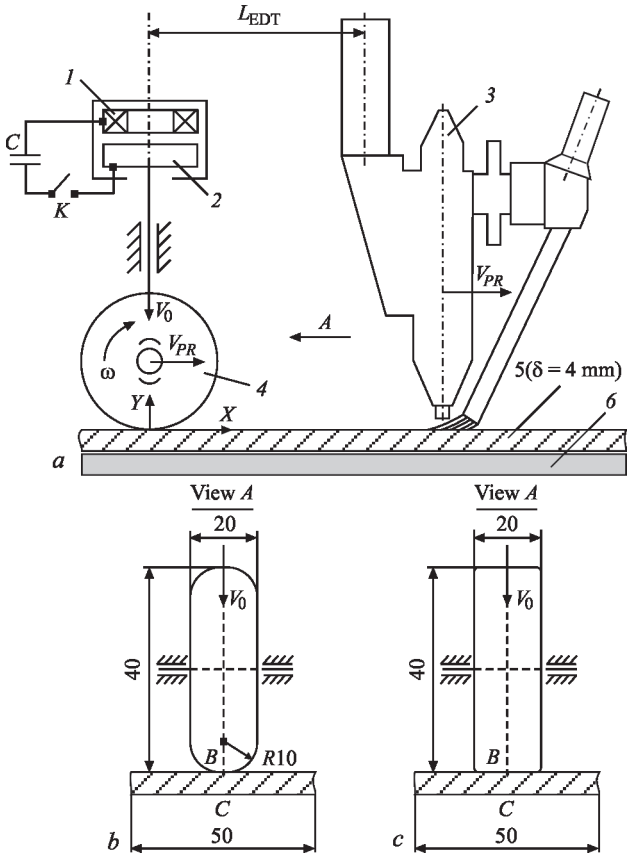

Figure 2. Process of EDT of plate metal after 3D printing: *a* — scheme of EDT process after 3D printing: *1* — inductor; *2* — disc; *3* — torch for 3D printing; *4* — indenter; *5* — plate for 3D printing with the thickness δ; *6* — working table; *C* — capacitor; *K* — contactor-switch; L_{EDT} — distance between the torch *3* and the indenter *4*; *X*, *Y* — axis of action of stresses; V_0 — line of electrodynamic pressure direction; V_{PR} — direction of 3D printing; ω — direction of rotation; *b* — geometric characteristics of the electrode-indenter with the contact surface in the form of a semicircle (EC), where B and C are the points along the line of V_0 respectively on the outer and back surfaces of the plate *5* (Figure 2, *a*); *c* — geometric characteristics of the electrode-indenter with the contact surface of a planar shape (EP), where *B* and *C* — similar to *b*)

$$\frac{d\rho}{dt}+\rho\left(\frac{\partial u}{\partial x}+\frac{\partial v}{\partial y}\right)=0, \qquad (1)$$

where *u*, *v* are the components of the velocity vector of the medium, m/s.

The equation of motion of the medium:

$$\rho\frac{du}{dt}=\frac{\partial\sigma_{xx}}{\partial x}+\frac{\partial\sigma_{xy}}{\partial y},\ \rho\frac{dv}{dt}=\frac{\partial\sigma_{yx}}{\partial x}+\frac{\partial\sigma_{yy}}{\partial y}, \qquad (2)$$

where σ_{ij} are the components of the stress tensor, Pa.

The energy equation E^* for a unit of mass:

$$\rho\frac{dE*}{dt}=\sigma_{xx}\dot{\varepsilon}_{xx}+\sigma_{yy}\dot{\varepsilon}_{yy}+2\sigma_{xy}\dot{\varepsilon}_{xy},$$

$$\dot{\varepsilon}_{xx}=\frac{\partial u}{\partial x},\quad \dot{\varepsilon}_{yy}=\frac{\partial v}{\partial y},\quad \dot{\varepsilon}_{xy}=\frac{1}{2}\left(\frac{\partial u}{\partial y}+\frac{\partial v}{\partial x}\right), \qquad (3)$$

where $\dot{\varepsilon}_{ij} = \frac{d\varepsilon_{ij}}{dt}$ are the components of the strain rate tensor, (s^{-1}).

To study the processes associated with large plastic deformations of the medium, finite deformations and the theory of plastic flow are used. This theory considers the plastic deformation of a solid body as a state of motion. The corresponding Prandtl–Reiss ratios can be written as:

$$\frac{dD_{\sigma_{xx}}}{dt} + 2G\dot{\lambda}D_{\sigma_{xx}} = 2G\left(\dot{\varepsilon}_{xx} + \frac{1}{3\rho}\cdot\frac{d\rho}{dt}\right), \quad (4)$$

$$\frac{dD_{\sigma_{yy}}}{dt} + 2G\dot{\lambda}D_{\sigma_{yy}} = 2G\left(\dot{\varepsilon}_{yy} + \frac{1}{3\rho}\cdot\frac{d\rho}{dt}\right), \quad (5)$$

$$\frac{dD_{\sigma_{xy}}}{dt} + 2G\dot{\lambda}D_{\sigma_{xy}} = 2G\dot{\varepsilon}_{xy}, \quad (6)$$

where G is the shear modulus, Pa; D_{ij} is the stress deviator components:

$$D_{ij} = \sigma_{ij} + p\delta_{ij},\ \delta_{ij} = 1\ (i = j),\ \delta_{ij} = 0\ (i \neq j), \quad (7)$$

where p is the average normal stress, Pa:

$$p = -\frac{\sigma_x + \sigma_y + \sigma_z}{3}.$$

The value of the specific power of plastic deformation is determined as:

$$\dot{\lambda} = \frac{3}{2Y^2}\sigma_{ij}\dot{\varepsilon}^p_{ij}, \quad \left(\frac{1}{\text{Pa}\cdot\text{s}}\right), \quad (8)$$

where Y is the dynamic yield strength of the material under study.

The system of equations is closed by the equation of the medium state in the form:

$$p = p(\rho, E). \quad (9)$$

In the mathematical setting, the behavior of the materials of the plate (aluminium AMg6 alloy) and electrode-indenter (copper M1) under the action of an external pulsed load was described using an ideal elastic-plastic rheological model of the material, which is available in the materials library of the ANSYS/LS-DYNA software. For this model, the value of the dynamic yield strength of material Y was accepted to be equal to the value of the yield strength σ_y. The corresponding values of the parameters of this model in the work were accepted as follows:

A plate with sizes of 500×500×4 mm of aluminium AMg6 alloy:

- density ρ = 2640 kg/m^3;
- modulus of elasticity E = 71 GPa;
- Poisson's ratio μ = 0.34;
- yield strength σ_y =150 MPa.

The electrode-indenter of M1 copper alloy with a mass of 102.5 g obtains three values of V_0, namely, 1, 5 and 10 m/s:

- density ρ = 8940 kg/m^3;
- modulus of elasticity E = 128 GPa;
- Poisson's ratio μ = 0.35;
- yield strength σ_y = 300 MPa.

Throughout the whole area of motion of an ideal-plastic medium, the ratio should be fulfilled, representing the Mises yield condition:

$$D^2_{\sigma_1} + D^2_{\sigma_2} + D^2_{\sigma_3} \leq \frac{2}{3}Y^2, \quad (10)$$

where D_{σ_1}, D_{σ_2} and D_{σ_3} are the main components of the stress deviator, Pa.

Thus, to evaluate the impact of EC and EP shape on the EDT efficiency of AMg6 alloy after 3D printing, numerical calculations of the process of their interaction with the plate at the contact speeds V_0 = 1, 5 and 10 m/s were carried out based on Prandtl–Reiss ratios. The value of V_0 was set based on the electrophysical characteristics of the capacitor C + inductor system (Figure 2, *a*), which are used for EDT [8].

MODELING RESULTS AND COMPARISON OF TECHNOLOGICAL APPROACHES

As a result of modeling, geometric characteristics of the cross-section of the deposited (printed layer 3) were established, Figure 1, which can be deformed by EDT in a one pass as a result of its contact interaction with the electrode-indenter (EC or EP) at different values of the speed V_0. The values of the height h_{PR} and width b_{PR} of the printed layer, subjected to EDT shaping during the period of the contact interaction t_{EDT} are given in Table 1.

The value of h_{PR} was determined as one, equal to the depth of the indentation as a result of a normal introduction of the indenter into the deposited layer at the point *B* (Figure 2, *b*, *c*) from its initial position to the position corresponding to the end of the contact. It was assumed that the value of h_{PR} of the layer, at which its deformation flush with the surface of the plate is guaranteed, should be not less than the depth of the indentation. The value of b_{PR} of the layer was determined as the distance from the impact line (axis *Y* in Figure 2, *a*) to the point that is located flush with the surface of the plate. The calculation of the values of h_{PR} and b_{PR}, which was carried out without taking into account the conditions of compressed or free plastic deformation [11], should be considered simplified. But the calculation results are sufficient for selecting the additive surfacing mode, which provides

Table 1. Parameters of contact interaction of the electrode and geometric characteristics of the deposited layer subjected to shaping by EDT

Number	Electrode shape	Electrode speed V_0, m/s	Contact duration t_{EDT}, μs	Layer height h_{PR}, mm	Layer width b_{PR}, mm
1	EP	1	74	0.016	0.53
2		5	86	0.168	1.89
3		10	102	0.451	3.06
4	EC	1	166	0.049	1.27
5		5	128	0.266	2.56
6		10	120	0.547	3.76

the required values of h_{PR} and b_{PR} of the printed layer, which can be subjected to EDT.

From the data in Table 1, it is seen that t_{EDT} between the layer and EP increases by 28 μs (38 %) with a rise in the initial speed of movement V_0 by an order. When using EC, on the contrary, an increase in V_0 to 10 m/s leads to a decrease in t_{EDT} by 46 μs (27 %). This is explained by the peculiarities in the energy exchange processes between the electrode-indenter and the plate. In accordance with an increase in the speed V_0, the kinetic energy grows, which during contact is converted into the energy of plastic deformation at the place of the contact, which affects the sizes of h_{PR} and b_{PR} of the compacted layer on the plate.

A rise in V_0 from 1 to 5 and up to 10 m/s increases the size of h_{PR} in both problem statements. At the same time, the values of h_{PR} and b_{PR} for EP increase by 10 and 3.6 times, respectively, when the speed grows to 5 m/s, and at V_0 = 10 m/s, the values of h_{PR} and b_{PR} increase by 2.5 and 1.6 times. At the same time, for EC, the growth is less rapid, the depth and width increase at V_0 = 5 m/s by 5.4 and 2 times, respectively, and at V_0 = 10 m/s they increase by another 2 and 1.4 times, respectively.

To evaluate the level of plastic deformations, the effective plastic deformations ε_{eff}^{p} were used, which represent a scalar value of the plastic component of the tensor of strain rate, which grows when the stress state is at the level of the yield strength. The values ε_{eff}^{p} were determined by the formula [10]:

$$\varepsilon_{eff} = \frac{\sqrt{2}}{3}\sqrt{(\varepsilon_1 - \varepsilon_2)^2 + (\varepsilon_2 - \varepsilon_3)^2 + (\varepsilon_3 - \varepsilon_1)^2}, \quad (11)$$

where ε_1, ε_2, ε_3 are the main deformations.

Although, an increase in the values of h_{PR} and b_{PR} for EP is more intensive, the absolute values of the geometric sizes of the compacted cross-section at the same speeds are greater for EC, which leads to a corresponding increase in the effective plastic deformations ε_{eff}^{p} and sizes of the plastic deformation zone (Figure 3). It should be noted that the boundaries of the plastic deformation zone, marked with an arrow, were determined under the condition that $\varepsilon_{eff}^{p} \geq 0.01$.

From Figure 1, it is seen that the zone of ε_{eff}^{p} distribution grows with an increase in V_0 and the shape of the distribution changes from a circle segment to a shape close to a trapezoid. The area of the plastic deformation zone increases faster during EC treatment (Figure 3, *b*). EDT at V_0 = 5 m/s does not deform the back surface of the metal when using EP (Figure 3, *a*) in contrast to the option of using EC (Figure 3, *b*). On the other hand, at the same V_0, it can be seen that the width of the deformation zone on the face surface at EC is 2 times larger than at EP. This proves the advantages of the shape EC over EP, as a technological tool for plastic deformation of metal of the next printed layer during additive surfacing.

Thus, the use of EDT at a speed of 1 m/s allows obtaining the surface effect of deformation with a segment radius with the center at the contact point of 0.7 and 1.6 mm size at EP and EC shapes of the electrode, respectively. When the speed increases to 5 m/s, EP provides a deformation zone with a radius of 2 mm, and EC forms a zone in the form of a trapezoid with a larger base on the face surface of 4 mm and a smaller base of 1.9 mm. An increase in V_0 up to 10 m/s leads to the creation of the plastic deformation zone of in the form of a trapezoid in both cases, with a larger and smaller base of 3.3 and 1.1 mm, respectively, at EP, and 6.2 and 4.7 mm, respectively, at EC.

Also, from Figure 1 it is seen, that as V_0 grows, not only the sizes of the plastic deformation zone increases, but also the values of ε_{eff}^{p} accordingly, it can be said here that when applying EP, the maximum values are formed on the contact surface of the printed layer with the electrode closer to the plane of symmetry. In the case of using EC, on the contrary, the peak values of ε_{eff}^{p} are shifted by 1.8–2.0 mm from the impact line (axis of symmetry) with the transition from the segmental shape of the deformation zone to the trapezoidal one. To compare the values of the maximum ε_{eff}^{p} and the values of ε_{eff}^{p} at the points *B* and *C* (Figure 2, *b*, *c*), located along the impact line, are given in Table 2.

Analyzing the data in Table 2 and Figure 1, it can be said that a growth of V_0 in the general case leads

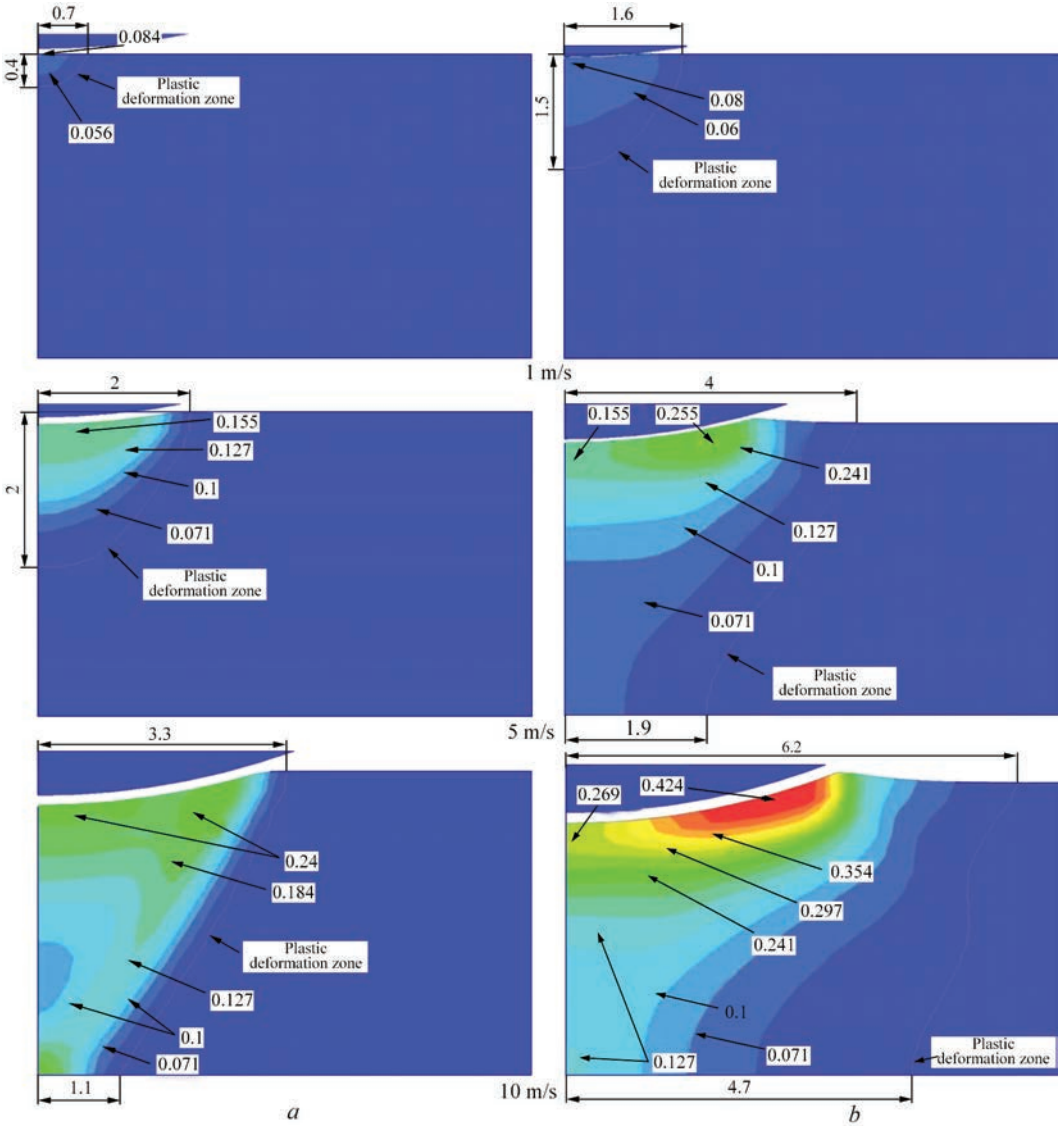

Figure 3. Calculated distribution of effective plastic deformations ε_{eff}^{p} along the OX axis along the line V_0 (Figure 2) in the plate after EDT EP (*a*) and after EDT EC (*b*) at the values of speed V_0 = 1, 5 and 10 m/s

to an increase in the maximum values of ε_{eff}^{p} regardless of the shape of the electrode. When using EP, an increase in V_0 from 1 to 5 m/s leads to an increase in the maximum ε_{eff}^{p} by 2.9 times, and a further increase to 10 m/s contributes to an increase by another 30 %. When using EC, the corresponding growth values are slightly higher: at 5 m/s — by 3.8 times, and at 10 m/s — by another 1.8. Thus, it can be seen that the use of the contact surface of EC contributes to a greater intensity of compaction at EDT than in EP.

The geometric characteristics of the deformation zone when using EC or EP have some differences. But if we consider the distribution of ε_{eff}^{p} at a speed of 1 m/s, then ε_{eff}^{p} concentrate on the face surface, and their values do not exceed 6 %, with a gradual decrease to zero along the impact line regardless of the shape of the electrode.

With an increase in V_0 to 5 m/s at EP, the distribution of ε_{eff}^{p} reaches the middle of the plate, but still has a superficial character with the maximum values on the contact surface being 17 % and a gradual decrease to almost zero on the back surface of the plate. The use of EC forms a trapezoidal deformation zone with the concentration of the maximum ε_{eff}^{p} at its edge with the value of up to 17.1 %. In this case, the value of ε_{eff}^{p} along the impact line gradually decreases from 15.1 % on the face surface to 3.8 % on the back one.

During treatment at V_0 = 10 m/s using EP, ε_{eff}^{p} have a trapezoidal distribution with the highest values on the back and face surfaces, from 22.4 to 20.5 %, respectively. In this case, the boundary of the plastic deformation zone represents almost a straight line, and the maximum values of ε_{eff}^{p} are at the point C. Also, at a distance of 2.5 mm from the face surface along the impact line, a local reduction in ε_{eff}^{p} to 8.5 % is observed, which should be taken into account when determining the critical zones of destruction when designing printed products. At the same time, the use of

Table 2. Values of effective plastic deformations ε_{eff}^{p}

Number	Electrode shape	Electrode-indenter speed, m/s	Maximum values ε_{eff}^{p}	ε_{eff}^{p} values on plate surfaces	
				Face (point *B*)	Back (point *C*)
1	EP	1	0.06	0.06	0
2		5	0.171	0.165	0.004
3		10	0.224	0.205	0.224
4	EC	1	0.063	0.04	0
5		5	0.239	0.151	0.038
6		10	0.424	0.260	0.116

EC at V_0 = 10 m/s determines the geometric shape of the deformation zone, which is qualitatively similar to the zone at V_0 = 5 m/s, but with a greater value of ε_{eff}^{p} — up to 42.4 %. At the same time, on the impact line, the values of ε_{eff}^{p} decrease from the point *B* to the point *C* from 26 to 11.6 %, respectively.

The distributions of ε_{eff}^{p} (Figure 3) are the result of the impact of the electrode shape at EDT on the overall intensity of plastic deformation of the metal, which characterizes its compaction at 3D printing. With the aim of more in-depth evaluation of the nature of the compaction of the printed metal, the distribution of ε_{x}^{p} and ε_{y}^{p} components along the axes *OX* and *OY* (Figure 2) of ε_{eff}^{p} deformation was calculated. The distribution of ε_{x}^{p} values determines the nature of deformation along the direction of V_{RR} printing (Figure 2), and the distribution of ε_{y}^{p} components along the impact line of V_0 (Figure 2). The distribution of ε_{x}^{p} components is shown in Figure 2.

Comparing ε_{x}^{p} for all cases, it is seen that with an increase in speed, the effect of the striker action on its distribution grows. At V_0 = 1 and 5 m/s, ε_{x}^{p} does not reach noticeable values at EP, but with an increase in V_0 to 10 m/s on the back surface at the point *C*, the deformation zone with the value more than 19 % ε_{x}^{p} is formed. In this case, the distribution of ε_{x}^{p} in the central up to cross-section has a form that is close to an isosceles triangle.

At the same time, at EC, a gradual increase in the intensity of deformation with an increase in V_0 from 1 m/s to 10 m/s is observed, where an accompanying increase in ε_{y}^{p} on the contact surface and in the zone near the symmetry axis (*Y*) is observed. At the same time, a zone of negative values up to –26 % is formed on the face surface on the boundary of the interaction surface of the plate with the electrode.

When considering the distribution of ε_{y}^{p} plastic deformation components, we have a more dynamic picture of the change in the process with a growing speed (Figure 5).

Considering the distribution of ε_{y}^{p} plastic deformation components at EP, the creation of a zone of negative values on the contact surface of the plate in the form of a circle segment is observed. With an increase in V_0, it grows over the plane and transforms into a trapezoid with the bases on the surfaces of the plate.

While analyzing the action of EC, the effect from the growth of speed is higher than when using EP. A transition from the zone of negative values on the contact surface in the form of a circle segment to a trapezoid-shaped zone at V_0 = 5 m/s and a rectangle at V_0 = 10 m/s is observed. The local zone of positive peak values at the border of the contact surface at V_0 = 1 m/s is absent, but becomes noticeable at V_0 = 5 and 10 m/s.

In order to analyze the distribution of values of stress state components over the thickness of the plate, the correpsonding calculated pictures of σ_x (Figure 6) and σ_y (Figure 7) distribution were constructed, which determine the characteristics of the printed metal during EDT with the use of EC or EP.

With an increase in the initial speed of the electrode-indenter, it is possible to conditionally see the trajectory of movement of compression and tension zones regarding the overall kinetics of changing the distribution of field σ_x and σ_y stress components. Thus, if we consider the distribution of σ_x at a speed of 1 m/s at EP (Figure 6, *a*), it is possible to see the origination of the tension zone along the plane of symmetry on the contact surface, behind which, the compression zone, and after it again the tension zone are created.

At a speed growth of up to 5 m/s, the extension of a near-surface tension area from the point of impact along the surface of the point *B* (Figure 2) is observed. In this case, the compressive stress zone extends to a half of the thickness of the plate, and across the width — behind the area of EP contact with a printed layer. The tension zones in the form of circle segments with the center in the point *C* (Figure 2) are formed on the back surface of the plate, where the peak value of σ_x reaches 76 MPa.

A growth in the speed of V_0 to 10 m/s leads to an increase in the surface tension zone across the thickness of the plate and in value. In this case, the compression stress zone decreases both by sizes and in

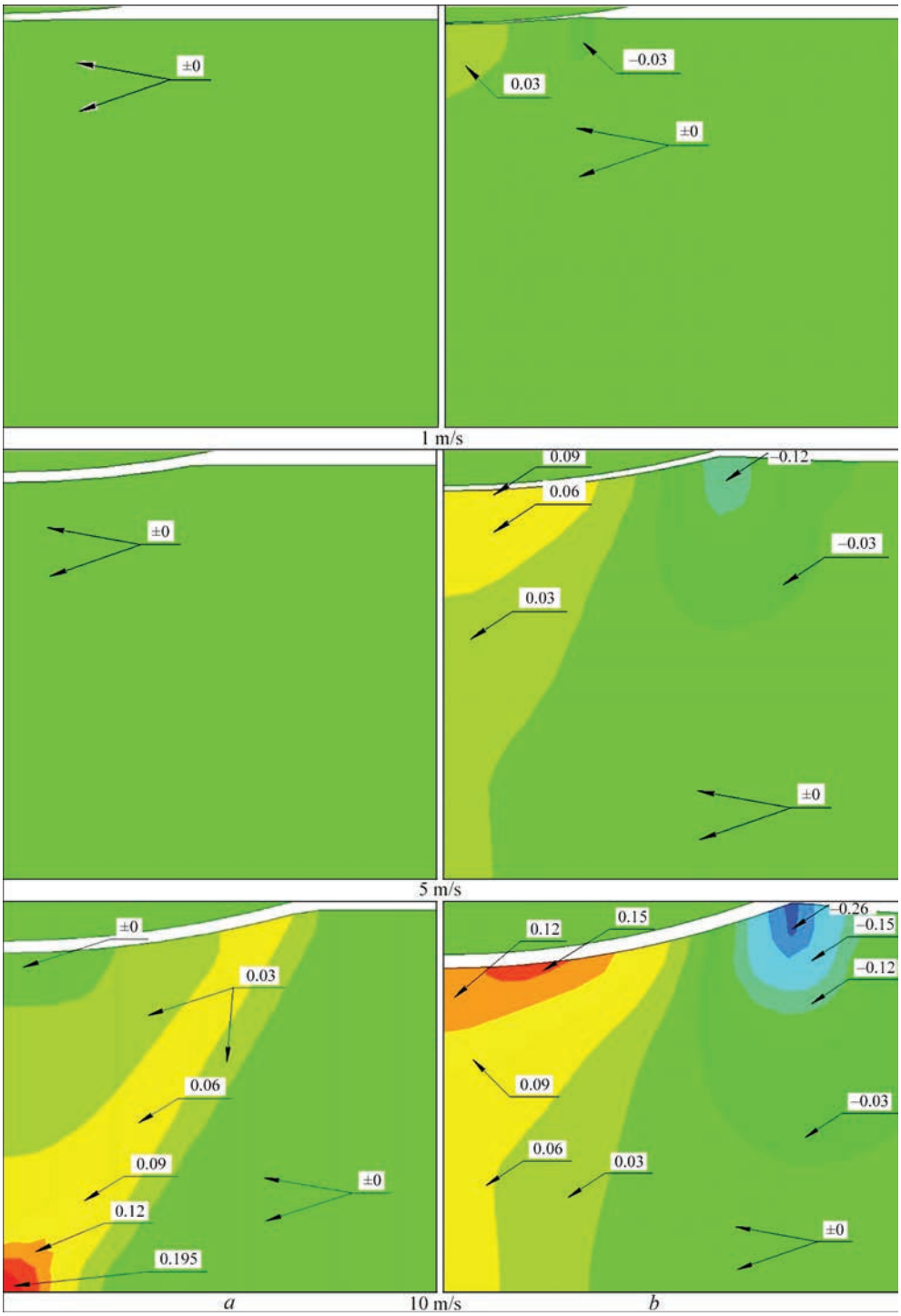

Figure 4. Calculated distribution of plastic deformations ε_x^p for the electrode shape of EP (*a*) and EC (*b*) at the initial speeds V_0 of the electrode of 1, 5 and 10 m/s

value, moving to the middle of the plate. At the same time, tensile stresses in the vicinity of the point *B* decrease and the geometric sizes of the zone decrease. The creation of a new compression zone on the back surface symmetrically to the surface tension zone is noted.

The plastic deformation of the deposited layer metal with the use of EC is more efficient (than with EP), because it leads to the dominance of σ_x compression zones throughout the area of action and values (compared to tension zones). At the same time, the value and area of distribution of compression σ_x grows with an increase in V_0.

At EDT by EC, already at V_0 = 1 m/s, a compression zone of about –200 MPa is created, which extends to the upper half of the thickness of the plate. The zone of the highest concentration of compression stresses with a peak value is at a depth of 1 mm from the face surface of the plate, and its width is equal to the width of the contact zone of EC with the metal. In the lower half of

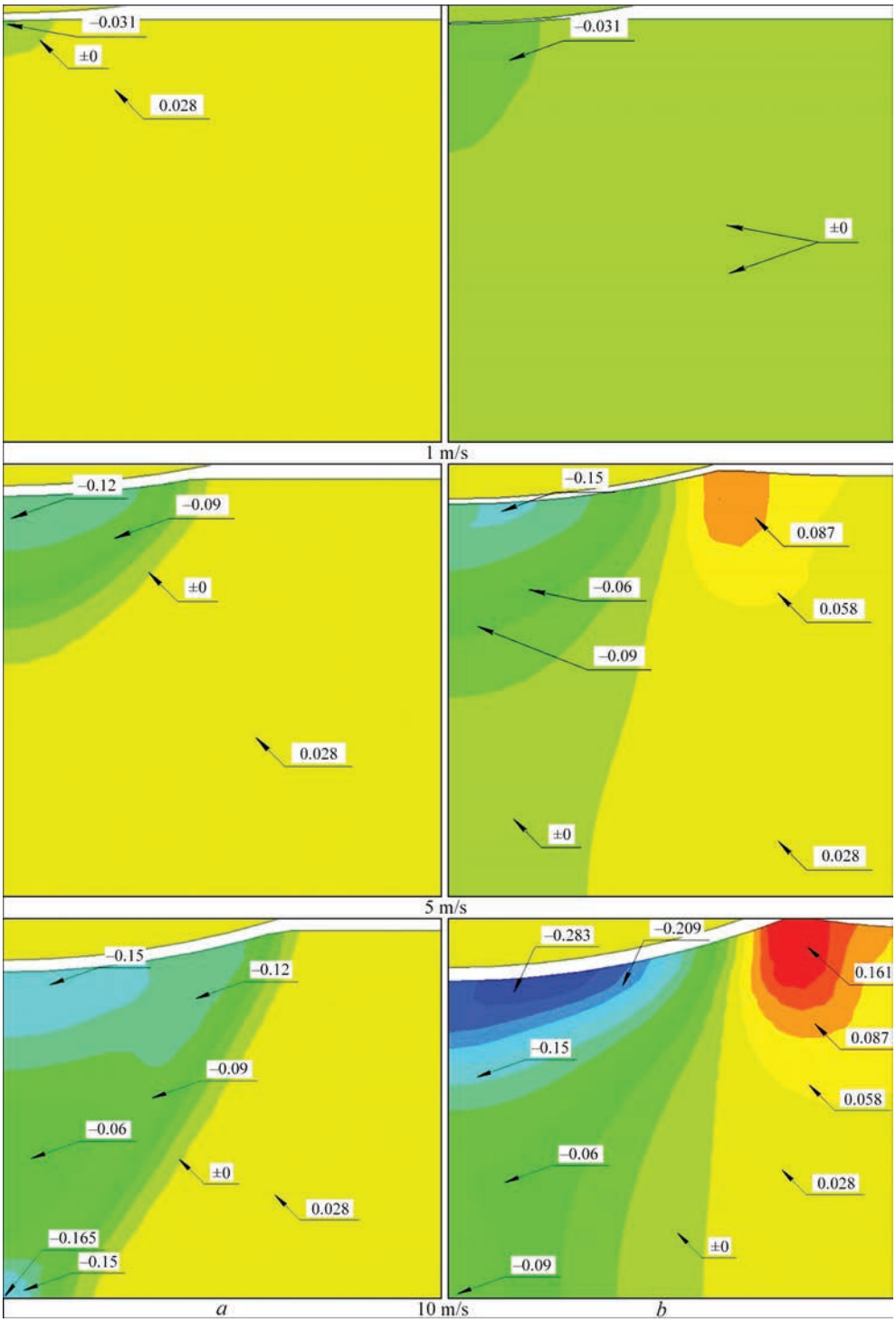

Figure 5. Calculated distribution of plastic deformations ε_y^p for the electrode shape of EP (*a*) and EC (*b*) at the initial speeds V_0 of the electrode of 1, 5 and 10 m/s

the thickness of the plate, the tension zone near the axis of symmetry is formed, the width of which also corresponds to the width of the contact zone. The maximum values of σ_x in this zone reach 25 MPa.

The growth of V_0 to 5 m/s throughout the whole thickness of the plate in the treatment zone forms a compression stress with two concentration zones. One of them is created in the form of a circle segment on the surface of the plate behind the edge of the contact zone, and the other is formed across the thickness of the plate with a uniform compression with the values close to the conditional yield strength $\sigma_{0.2}$ of AMg6 alloy (150 MPa).

The use of EC at V_0 = 10 m/s leads to an increase in the compression stresses to –200 MPa behind the contact zone. In this case, the compression zone in the thickness of the plate is shifted in its minimum to the point *C*, where peak values reach –200 MPa.

At the same time, the distribution of σ_y has its own features, which are shown in Figure 7. In general con-

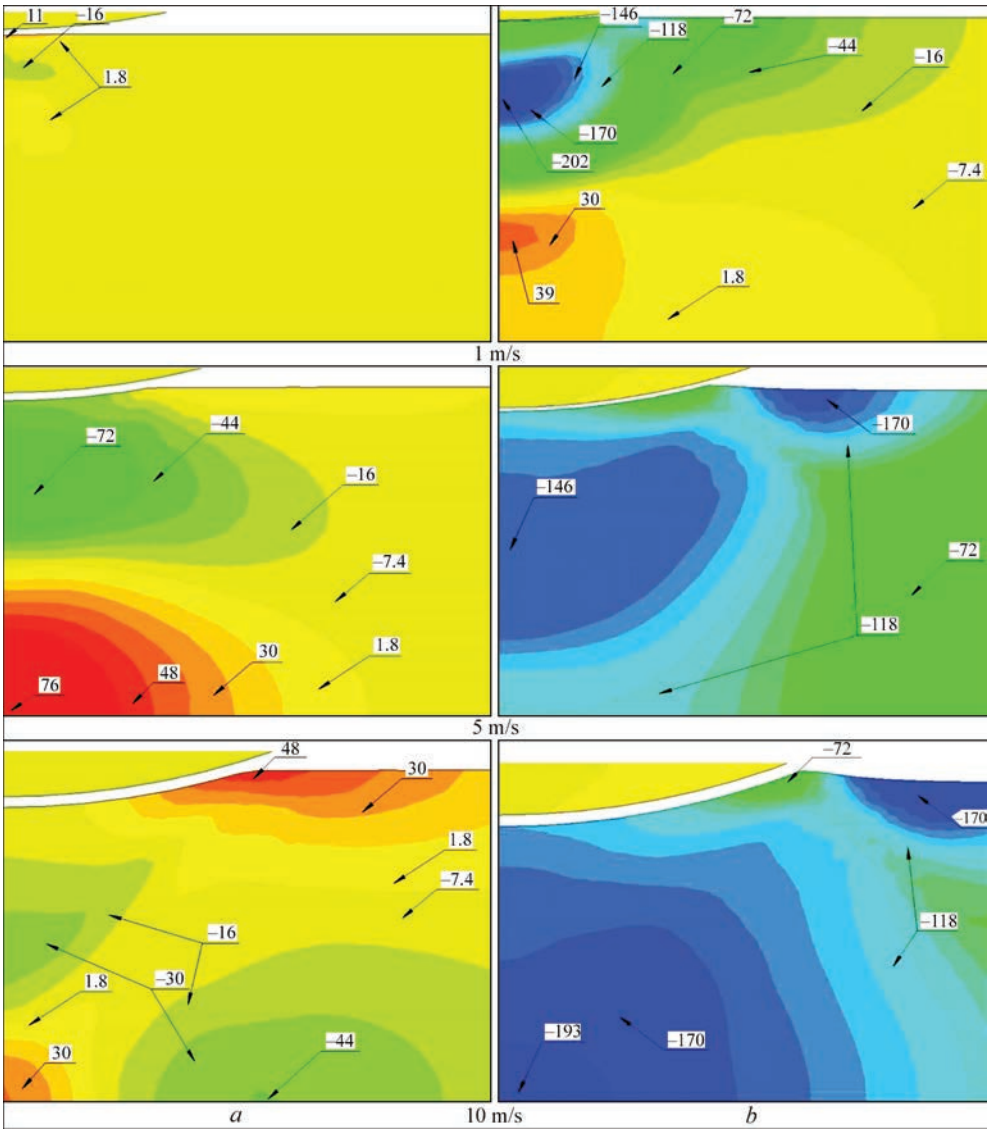

Figure 6. Distribution of residual σ_x stresses (MPa) as a result of EDT using EP (*a*) and EC (*b*) at the initial speeds V_0 of the electrode of 1, 5 and 10 m/s

sideration of evolution of σ_x stress component in EDT with the use of EP, a transition from a slight change in the stress state at V_0 = 1 m/s to the formation of two pronounced tension and compression zones at an increase in the speed to 5 and 10 m/s is observed. The tension zone, which is created at the peak at the point *C*, is similar to a rectangle with an elongated angle in the direction of the dent boundary. The compression zone, formed behind the tension zone, has a shape similar to a triangle with a base on the back surface and the vertex, which with an increase in the speed approaches the dent edge. At V_0 = 5 and 10 m/s, no significant changes in the stress state on the face surface compared to the state at V_0 = 1 m/s is observed.

When considering the distribution, the stress σ_y components in EDT with the use of EC, the formation of alternate tension and compression zones is also observed. The compression zone is created under the dent surface in the form of a circle segment, the outer radius of which reaches a half of the thickness of the plate at V_0 = 1 m/s. At V_0 = 5 and 10 m/s, the area of the compression zone extends to the entire thickness of the plate, and reaches the dent edge across its width, reducing the area of the tension zone and moving it from the impact line. At the same time, with an increase in speed, the shape of the tension zone is converted into a pointed strip with the edge vertex near the dent edge.

The results of the calculation of the values of σ_x and σ_y residual stress components at the reference points along the impact line are summarized in Tables 3 and 4.

Based on the data of Table 3, it can be seen that σ_x component at V_0 = 1 m/s when using EP is exclusively tensile and at EC acquires a negative sign already in the upper half of the thickness of the plate. At the same time, due to intensive plastic deformation, the values of σ_x stresses at EC at V_0 = 1 m/s reach 202 MPa, i.e.

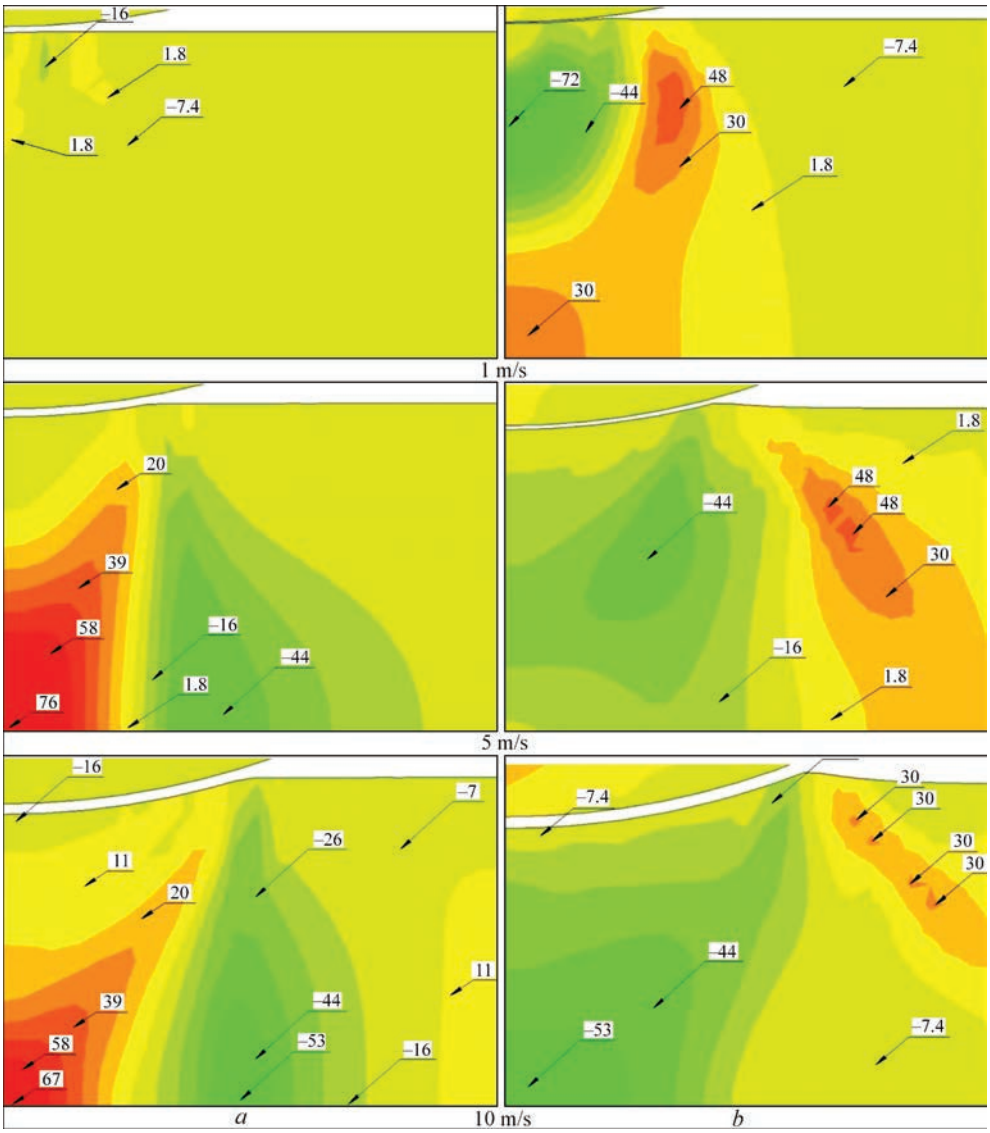

Figure 7. Distribution of values of residual σ_y stresses (MPa) as a result of EDT using EP (*a*) and EC (*b*) at the initial speeds V_0 of the electrode of 1, 5 and 10 m/s

they are behind the elasticity limit on the local area under the contact surface (at a point at a distance of 1 mm from the surface).

In the range of V_0 = 5–10 m/s, the values of σ_x acquire a negative sign on the upper half of the plate when applying EP and are exceptionally negative when using EC. Also, at V_0 = 5–10 m/s when using EP, the compression σ_x values on the upper half of the plate are close to tensile σ_x on the lower one.

During an increase in V_0, the use of EC allows increasing the value of compression σ_x stresses and their distribution zone. The compression stresses reach the values close to the yield strength of the material over the entire thickness of the metal.

Analyzing the distributions of σ_x component (Table 4), it should be noted that the value of this stress component is significantly lower compared to σ_y. Thus, when applying EP, the effect on the face half of the plate along the impact line is minimal regardless of the speed. At the same time, at speeds of 5 and 10 m/s, an increase in tensile stresses on the back half of the plate of up to 78 MPa is observed.

The use of EC throughout the whole speed range initiates the formation of compression σ_y stresses within –5– –36 MPa, except for the point at a thickness of

Table 3. Calculated values of residual stress state σ_x components (in MPa) over the thickness of the plate (from the point *B* to the point *C* (see Figure 2))

Electrode shape	V_0, m/s	Point coordinate over the thickness of the plate (along the impact line), mm				
		0 (point *B*)	1	2	3	4 (point *C*)
EP	1	15	4	1	0	0
	5	–25	–61	–2	59	76
	10	–6	–7	–16	13	32
EC	1	–29	–202	–16	21	13
	5	–133	–160	–164	–153	–128
	10	–147	–163	–166	–177	–180

Table 4. Calculated values of residual stress state σ_y components (in MPa) over the thickness of the plate (from the point *B* to the point *C* (see Figure 2))

Electrode shape	V_0, m/s	Point coordinate over the thickness of the plate (along the impact line), mm				
		0 (point *B*)	1	2	3	4 (point *C*)
EP	1	–7	2	0.5	0	0
	5	0.1	0.1	23	61	78
	10	0.1	5	12	40	60
EC	1	–5	–79	–24	21	21
	5	0	–12	–18	–17	–7
	10	–3	–20	–25	–36	40

1 mm from the face surface at a speed of treatment of 1 m/s, where σ_y = –79 MPa. But on the back side, a localized tension zone of up to 40 MPa is formed.

Based on the abovementioned comparisons of values of stress state components along the impact line (Tables 3, 4), it should be noted that, unlike the shape of the electrode-indenter EP, the use of EC shape leads to the formation of almost uniform distribution of both stress components (σ_x and σ_y) across the thickness of the deposited layer. In addition, the use of EP leads to the formation of both compression stresses, as well as more dangerous tensile stresses with the values that can reach half of the value of the material yield strength. Whereas, the use of EC leads to the formation of both σ_x and σ_y compression stress components, the values of which can reach the yield strength of the material. As was shown in [12–14], such distribution of plastic deformations contributes to refinement of the metal structure, and the resulted distribution of components of compression stresses facilitates an increase in the resistance to the destruction of products in the conditions of fatigue loads.

Thus, by combining electrodynamic treatment with additive surfacing, an improvement in the physical and mechanical characteristics of the material of metal products in 3D printing technologies can be expected.

CONCLUSIONS

1. Based on the Prandtl–Reiss ratio, numerous experiments on studying the effectiveness of the influence of the shape of the contact surface of the electrode-indenter for electrodynamic treatment of the deposited layer in the technologies of additive surfacing on the distribution of components of plastic deformations and residual stresses in it were carried out.

2. It was established that the use of the copper electrode-indenter in the form of a roller with a contact surface in the form of a semicircle (EC) for EDT compared to the electrode with a contact surface in the form of a straight line (EP), which moves under the same conditions, results in:

● an increase in the duration of the contact with the deposited layer treated by 50 % and, as a result of this, the sizes of the depth and width of the layer increase by 55 and 35 %, respectively;

● distribution of the deposited layer of the zone of effective plastic deformations, having a shape close to trapezoid, across the entire thickness (in the case of EP, the zone of ε_{eff}^{p} extends only to a half of the thickness of the plate and has a shape of a circle segment), and the values of maximum deformations at EC are 1.4 times higher than the action of EP;

● formation of almost uniform distribution of both stress state σ_x and σ_y components over the thickness of the plate, which, unlike EP, are the compression stresses, the values of which can reach the yield strength of AMg6 alloy.

3. The results of the mathematical modeling give reason to use the shape of the electrode-indenter — EC for the development of combined technologies of 3D printing of volumetric metal products, which consist in the combination of layered (additive) surfacing (WAAM, plasma, microplasma surfacing, etc.), a volumetric product with electrodynamic treatment of each deposited layer.

The work was performed with the support of the following projects:

● *The National Key Research and Development Program of China (grant number 2020YFE0205300).*

● *GDAS'Project of Science and Technology Development (2020GDASYL-20200301001), China.*

REFERENCES

1. Peleshenko, S., Korzhyk, V., Voitenko, O. et al. (2017) Analysis of the current state of additive welding technologies for manufacturing volume metallic products (review). *Eastern European J. of Enterprise Technologies*, **87**, 42–52. DOI: https://doi.org/10.15587/1729-4061.2017.99666
2. Kvasnytskyi, V., Korzhyk, V., Lahodzinkyi, I. et. al. (2020) Creation of Volumetric Products Using Additive Arc Cladding with Compact and Powder Filler Materials. In: *Proc. of the 2020 IEEE 10th Inter. Conf. on Nanomaterials: Applications and Properties (Sumy, Ukraine, 9–13 Nov. 2020)*, 02SAMA16-1-02SAMA16-5, DOI: https://doi.org/10.1109/NAP51477.2020.9309696
3. Soshi, M. (2017) Innovative grid molding and cooling using an additive and subtractive hybrid CNC machine tool. *CIRP Annals – Manufacturing Technology*, 66(**1**), 401–404.
4. Dongqing, Yang, Gang, Wang, Guangjun, Zhang (2017) Thermal analysis for single-pass multi-layer GMAW based additive manufacturing using infrared thermography. *J. Materials Proc. Technology*, **244**, 215–224.
5. Trufyakov, V.I. (1973) *Fatigue of welded joints.* Kyiv, Naukova Dumka [in Russian].
6. Lobanov, L.M., Pashchyn, N.A., Kondratenko, I.P. et al. (2018) Development of post-weld electrodynamic treatment using electric current pulses for control of stress-strain states and improvement of life of welded structures. *Materials*

Performance and Characterization, **7**(**4**). DOI: https://doi.org/10.1520/MPC20170092
7. Lobanov, L.M., Korzhyk, V.M., Pashchyn, M.O. et al. (2022) Deformation-free TIG welding of AMg6 alloy with application of electrodynamic treatment of weld metal. *The Paton Welding J.,* **8**, 3–8. DOI: https://doi.org/10.37434/tpwj2022.08.01
8. Lobanov, L.M., Pashchyn, M.O., Mikhodui, O.L. et al. (2017) Effect of the indenting electrode impact on the stress-strain state of an AMg6 alloy on electrodynamic treatment. *Strength of Materials*, 49(**3**), 369–380.
9. Sidorenko, Y.M., Shlenskii, P. (2013) On the assessment of stress-strain state of the load-bearing structural elements in the tubular explosion chamber. *Strength of Materials*, 45(**2**), 210–220.
10. Lobanov, L.M., Pashchyn, M.O., Mikhodui, O.L. et al. (2022) Influence of electrode shape on stress-strain state of AMg6 alloy during its electrodynamic treatment. *The Paton Welding J.,* **9**, 3–10. DOI: https://doi.org/10.37434/as2022.09.01
11. Johnson, K. (1989) *Mechanics of contact interaction.* Moscow, Mir [in Russian].
12. Lobanov, L.M., Pashchin, N.A., Solomijchuk, T.G. (2012) Changes of structure of aluminium alloy AMg6 in the zone of electrodynamic actions. *Visnyk Ukr. Materialoznavchogo Tovarystva,* **5**, 30–42 [in Russian].
13. Lobanov, L.M., Pashchin, E.N., Berdnikova, E.N. (2015) Influence of electrodynamic treatment on features of fracture mictomechanism of aluminium alloy AMg6 at cyclic loading. *Visnyk Ukr. Materialoznavchogo Tovarystva,* **8**, 27–37 [in Russian].
14. Lobanov, L.M., Pashin, N.A., Timoshenko, N. et. al. (2017) Effect of the electrodynamic treatment on the life of AMg6 aluminium alloy weld joints. *Strength of Materials*, 49(**2**), 234–238. DOI: http://dx.doi.org/10.1007/s11223-017-9862-8

ORCID
L.M. Lobanov: 0000-0001-9296-2335,
V.M. Korzhyk: 0000-0001-9106-8593,
M.O. Pashchyn: 0000-0002-2201-5137,
O.L. Mikhodui: 0000-0001-6660-7540,
P.R. Ustymenko: 0000-0002-5318-2675,
A.O. Alyoshyn: 000-001-9696-6800

CONFLICT OF INTEREST
The Authors declare no conflict of interest

CORRESPONDING AUTHOR
M.O. Pashchyn
E.O. Paton Electric Welding Institute of the NASU
11 Kazymyr Malevych Str., 03150, Kyiv, Ukraine.
E-mail: svarka2000@ukr.net

SUGGESTED CITATION
L.M. Lobanov, V.M. Korzhyk, M.O. Pashchyn, O.L. Mikhodui, P.R. Ustymenko, Zhang Yupeng, A.O. Alyoshin, O.M. Voitenko (2023) Mathematical modeling of the impact of electrodynamic treatment in the process of additive surfacing on the stress-strain state of volumetric products from aluminium-magnesium alloy. *The Paton Welding J*., **7**, 3–14.

JOURNAL HOME PAGE
https://patonpublishinghouse.com/eng/journals/tpwj

Received: 14.06.2023
Accepted: 06.09.2023